# Stimulus selectivity and response latency in putative inhibitory and excitatory neurons of the primate inferior temporal cortex

**Ryan E. B. Mruczek and David L. Sheinberg**

*J Neurophysiol* 108:2725-2736, 2012. First published 29 August 2012; doi:10.1152/jn.00618.2012

*J Neurophysiol* 108: 2725–2736, 2012.
First published August 29, 2012; doi:10.1152/jn.00618.2012.

# Stimulus selectivity and response latency in putative inhibitory and excitatory neurons of the primate inferior temporal cortex

**Ryan E. B. Mruczek and David L. Sheinberg**
*Department of Neuroscience, Brown University, Providence, Rhode Island*

Submitted 17 July 2012; accepted in final form 27 August 2012

**Mruczek RE, Sheinberg DL.** Stimulus selectivity and response latency in putative inhibitory and excitatory neurons of the primate inferior temporal cortex. *J Neurophysiol* 108: 2725–2736, 2012. First published August 29, 2012; doi:10.1152/jn.00618.2012.—The cerebral cortex is composed of many distinct classes of neurons. Numerous studies have demonstrated corresponding differences in neuronal properties across cell types, but these comparisons have largely been limited to conditions outside of awake, behaving animals. Thus the functional role of the various cell types is not well understood. Here, we investigate differences in the functional properties of two widespread and broad classes of cells in inferior temporal cortex of macaque monkeys: inhibitory interneurons and excitatory projection cells. Cells were classified as putative inhibitory or putative excitatory neurons on the basis of their extracellular waveform characteristics (e.g., spike duration). Consistent with previous intracellular recordings in cortical slices, putative inhibitory neurons had higher spontaneous firing rates and higher stimulus-evoked firing rates than putative excitatory neurons. Additionally, putative excitatory neurons were more susceptible to spike waveform adaptation following very short interspike intervals. Finally, we compared two functional properties of each neuron's stimulus-evoked response: stimulus selectivity and response latency. First, putative excitatory neurons showed stronger stimulus selectivity compared with putative inhibitory neurons. Second, putative inhibitory neurons had shorter response latencies compared with putative excitatory neurons. Selectivity differences were maintained and latency differences were enhanced during a visual search task emulating more natural viewing conditions. Our results suggest that short-latency inhibitory responses are likely to sculpt visual processing in excitatory neurons, yielding a sparser visual representation.

inferotemporal cortex; monkey; interneuron; pyramidal cell; object recognition

BEGINNING WITH the pioneering studies of Hubel and Weisel (1968), our understanding of the functional properties of neurons in primate visual cortex has been primarily advanced by single-unit extracellular recordings. While these studies have greatly expanded our knowledge of neuronal response properties, they have largely ignored the vast diversity of cell types known to exist in cortex (Ramón y Cajal 1899). In vitro studies have established that morphology, gene expression, and membrane properties vary widely across cell type (Markram et al. 2004; Peters and Jones 1984; Toledo-Rodriguez et al. 2003). Although these differences have a direct consequence on how neurons transmit information through patterns of action potentials, they have been typically overlooked in experiments involving extracellular recordings and awake, behaving animals.

Address for reprint requests and other correspondence: D. L. Sheinberg, Box GL-N, Dept. of Neuroscience, Brown Univ., Providence, RI 02912 (e-mail: david_sheinberg@brown.edu).

Cortical neurons can be broadly classified as inhibitory or excitatory, depending on their primary synaptic neurotransmitter. Intracellular recordings in cortical slices have established that GABAergic inhibitory interneurons produce shorter-duration action potentials than glutamatergic excitatory pyramidal cells (Connors and Gutnick 1990; McCormick et al. 1985; Nowak et al. 2003). This is likely the result of differences in the kinetics of the expressed sodium and potassium channels in each cell type (Martina and Jonas 1997; Martina et al. 1998; McBain and Fisahn 2001). Henze et al. (2000) demonstrated that the extracellular waveform is defined by specific properties of the intracellular waveform, such as duration and amplitude changes. This makes it possible to broadly classify extracellularly recorded cells as putative inhibitory or putative excitatory based on their spike duration. Such a scheme is supported by additional studies that have concurrently identified either excitatory projection neurons by antidromic stimulation (Johnston et al. 2009) or inhibitory interneurons by pairwise recordings and cross-correlation analysis (Bartho et al. 2004; Tamura et al. 2004).

A number of recent studies employing waveform-based classification have contributed to our understanding of the different functional roles played by excitatory and inhibitory neurons in visual cortex (Chen et al. 2008; Gur et al. 1999; Mitchell et al. 2007; Woloszyn and Sheinberg 2012), somatosensory cortex (Mountcastle et al. 1969), prefrontal cortex (Constantinidis and Goldman-Rakic 2002; Diester and Nieder 2008; Hussar and Pasternak 2009, 2012; Johnston et al. 2009; Rao et al. 1999; Wilson et al. 1994), and the hippocampus (Csicsvari et al. 1999), among others. Even the most basic functional properties are likely to differ across cell type, and understanding these differences may shed light on the local interactions that take place within cortical networks. Here, we report on two basic response properties of putative inhibitory and putative excitatory neurons in inferior temporal cortex: stimulus selectivity and response latency. Briefly, putative excitatory neurons showed stronger stimulus selectivity, while putative inhibitory neurons showed shorter response latencies. These differences were apparent in the initial transient response to abrupt stimulus onsets and when images were freely selected for fixation during a visual search task. Earlier and less selective response profiles for putative inhibitory neurons are consistent with the hypothesis that local inhibitory connections play a key role in shaping the neural response profiles of excitatory neurons in inferior temporal cortex (Wang et al. 2000).

## MATERIALS AND METHODS

The experimental apparatus, recording methods, and behavioral tasks are described in detail elsewhere (Mruczek and Sheinberg 2007a, 2007b; Sheinberg and Logothetis 2001).

*Animals, surgery and recording techniques.* Four adult male rhesus monkeys (*Macaca mulatta*; *monkeys M*, *S*, *Q*, and *V*) were the subjects in this study.[1] Each monkey had a recording chamber implanted over one hemisphere (left for *monkeys M* and *S*, right for *monkeys Q* and *V*; Horsley-Clark coordinates: 15–20 anterior, 16–20 lateral) and a titanium head post for head restraint. All surgeries were performed with sterile technique while the animals were intubated and anesthetized with isoflurane gas. Animal protocols were reviewed and approved by the Brown University Institutional Animal Care and Use Committee (IACUC), and all procedures conformed to the National Research Council *Guide for the Care and Use of Laboratory Animals* and the US Public Health Service *Policy on Humane Care and Use of Laboratory Animals*, as adopted by the Society for Neuroscience in its *Policy on the Use of Animals in Neuroscience Research*.

During each recording session, a single electrode was advanced through a guide tube inserted to a level just below the dura (*monkey S*) or through a chronic guide tube (*monkeys M*, *Q*, and *V*). For *monkeys M* and *S*, electrodes were composed of a tungsten core with a glass coating (Alpha-Omega). Neural signals were amplified (model A-1, BAK Electronics, Germantown, MD), filtered (model 3364, Krohn-Hite, Brockton, MA; 100 Hz to 12 kHz), and digitized at 34 kHz. For *monkeys Q* and *V*, electrodes were composed of a PtIr core (90/10; A-M Systems, Sequim, WA) with a glass coating. Neural signals were amplified (model A-1, BAK Electronics), filtered (Krohn-Hite; 100 Hz/12 dB to 8 kHz/24 dB), and digitized at 22 kHz. For all monkeys, electrodes were advanced with a micro-positioner (David Kopf Instruments, Tujunga, CA).

Eye movements were recorded with an EyeLink II video eye tracking system (*monkeys M* and *S*; SR Research, Mississauga, ON, Canada) running at 500 Hz or a scleral search coil (*monkeys Q* and *V*; Robinson 1963). Eye movement signals were sampled by the control system at 1 kHz, and a moving average was stored to disk every 5 ms (200 Hz).

*Neuron selection and spike extraction.* Inferior temporal cortex was located based on the stereotaxic placement of the recording chamber and by counting white-gray matter transitions. Spikes were extracted off-line from the stored analog signal with a threshold and two time-amplitude discrimination windows (custom software). For each spike, we obtained a 4-ms trace, spanning 1 ms before to 3 ms after the threshold crossing. This window was sufficient to capture the full waveform (i.e., the trace reached 5% of its baseline amplitude after repolarization) of every cell in our data set. To facilitate the comparison of waveform characteristics across cells, we inverted the trace of some cells such that all spikes in our data set displayed an initial upward-going phase (i.e., peak) followed by a downward-going phase (i.e., trough; see Fig. 1).

All spikes in the present data set displayed a high signal-to-noise ratio (median = 29.7; range = 5.6–159.9), defined as the average peak-to-trough amplitude of each spike divided by twice the mean absolute amplitude of the recorded trace in a 200-$\mu$s window starting 1 ms prior to the start of each spike. Additionally, all cells in the present data set had a minimum interspike interval of 1.2 ms. A representative spike trace from a neuron with a signal-to-noise ratio of 51.0 can be seen in Fig. 2*C*. The present data set is composed of 322 neurons (42 from *monkey M*, 97 from *monkey S*, 111 from *monkey Q*, and 72 from *monkey V*).

*Stimuli, display, and task descriptions.* Stimuli were presented on a dedicated graphics workstation running an OpenGL-based stimulation program. Behavioral control for the experiments was maintained by a network of interconnected PCs running the QNX real-time operating system (QNX Software Systems, Ottawa, ON, Canada). Experimental control and the collection of behavioral measures were conducted with custom-written programs. All behavioral data, such as button responses and eye position signals, were available for online monitoring and stored to disk for off-line analysis.

For behavioral trials, the stimulus set contained full-color images of everyday objects and scenes (Hemera Photo-Objects, Gatineau, QC, Canada; Corel, Ottawa, ON, Canada). Objects subtended $\sim$1.5 $\times$ 1.5°. All stimuli used were highly familiar to the monkeys.

As a precursor to a visual search task (described below) monkeys performed a screening task in order to identify a set of stimuli eliciting a particular response profile from the recorded cell (see Mruczek and Sheinberg 2007a, 2007b; Sheinberg and Logothetis 2001). During the screening task, monkeys were presented with isolated objects on a uniform gray (50%) background while they performed either a passive-viewing task (*monkeys M* and *S*) or a classification task (*monkeys Q* and *V*). During the passive-viewing task, the monkey initiated trials by fixating a small spot at the center of the screen for 500 ms. After acquisition, the fixation spot was extinguished and three to eight isolated stimuli were presented sequentially at the center of the screen for 200–600 ms with a 200- to 600-ms interstimulus interval. At the end of the stimulus period a second fixation spot was presented in a randomly selected location 6° above, below, left, or right of the center of the screen. The monkey was required to fixate the second spot to receive juice reinforcement. For the classification task, the monkey was initially required to fixate the center (3° window) of a blank screen for 300 ms, after which a single object appeared centrally. The monkey's task was to press a lever (left or right) that had previously been associated with that object. Correct choices were immediately followed by delivery of a juice reward and removal of the stimulus from the screen. Feedback was also provided by auditory cues indicating correct and incorrect trials. There were no explicit constraints on the monkey's eye movements during the time that the visual display was present, but the analysis windows for selectivity and latency measures were limited to the time of the initial transient response from the neurons (see below). Additionally, trials in which the monkey made a saccade that was not corrective (i.e., small saccades that landed on the image) were excluded from all functional analyses (2.1% for *monkey M*, 0.6% for *monkey S*, 9.1% for *monkey Q*, and 4.1% for *monkey V*). Small-amplitude saccades, such as microsaccades, have little influence on the activity of inferior temporal cortex neurons under normal conditions (Leopold and Logothetis 1998).

For the visual search task, monkeys were presented with a search array containing one target stimulus and 30 distractor stimuli on a uniform gray (50%) background (Mruczek and Sheinberg 2007a), 2 distractor stimuli on a noise background that consisted of pseudorandomly colored squares (Mruczek and Sheinberg 2007b), or embedded within a natural scene (Sheinberg and Logothetis 2001). In all cases, the monkey's task was to locate any known target image and press the button/lever (left or right) that had previously been associated with that target. Correct choices were immediately followed by delivery of a juice reward and removal of the stimulus array from the screen. Feedback was also provided by auditory cues indicating correct and incorrect trials. Note that there were no explicit constraints on the monkeys' eye movements during the time that the visual display was present. Rather, the monkeys were allowed to freely explore the display.

Spikes recorded in the absence of any specific task were included only for analyses that were not stimulus- or task dependent (e.g., waveform properties and short interspike interval analysis, see below).

*Data analysis and statistics.* All spikes recorded from a given cell were averaged to obtain the spike waveform. We used two independent methods to classify neurons as putative inhibitory or putative excitatory. For the spike width classification, spike width was defined as the time from the waveform peak to the waveform trough (see Fig. 1*A*, *inset*). The distribution of spike widths was tested for departure from unimodality with Hartigan's dip test (Hartigan and Hartigan 1985) and a permutation test (100,000 permutations). We modeled the

[1] Note that *monkey S* in the present study is the same subject as *monkey S* in the Mruczek and Sheinberg (2007a) studies and *monkey V* in the present study is the same as *monkey S* in the Sheinberg and Logothetis (2001) study.

distribution of spike widths as a sum of two Gaussian distributions and chose the local minimum of the combined distribution (352 $\mu$s) as the cutoff for our classification.

For the second classification method, we performed *k*-means clustering ($k = 2$, distance metric = 1 − Pearson correlation) of the full spike waveform vectors. For this analysis, the waveforms were first normalized by their peak amplitude and aligned to the time of the peak to remove irrelevant features related to the spike-extraction process (Diester and Nieder 2008).

For both methods, the group of neurons with the shorter waveform durations was deemed putative inhibitory. The majority of the analyses presented here included only those neurons that were consistently classified by both methods, with inconsistently classified neurons considered separately.

Spontaneous and stimulus-evoked firing rates were calculated for the sudden-onset condition of the screening tasks described above. Spontaneous firing rates were measured in a 150-ms time window prior to the onset of the stimulus. Stimulus-evoked responses were measured in a 150-ms time window starting 50 ms after stimulus onset.

To quantify waveform adaptation, we compared the amplitude of the spike trough (i.e., minimum of second phase) for pairs of spikes that occurred with very short interspike intervals. For this analysis, we only considered pairs of spikes that occurred within 8 ms of each other, with no preceding spikes for at least 50 ms. Note that with this second criterion, no single spikes could be included as the first and second spike in two different pairs of spikes. For each neuron with at least five such spike pairs, the average waveform for the first spike and second spike in each pair was calculated separately. We then defined an amplitude adaptation index (AI) as follows:

$$AI_{amp} = (Amp_1 - Amp_2)/(Amp_1 + Amp_2)$$

where $Amp_1$ is the amplitude of the trough for the average first spike waveform and $Amp_2$ is the amplitude of the trough for the average second spike waveform. This value ranges from −1 to 1, with positive values indicating decreased trough amplitudes for the second spike. Similar adaptation indexes were calculated for peak-to-trough slope and peak-to-trough duration.

Measurements of stimulus selectivity were limited to data collected during the very first block of trials from the screening task for each neuron. This ensured that the stimuli were selected randomly and without any potential experimenter bias, since the end-goal of this screening process was to identify a small subset of stimuli that evoked a specific response profile from the recorded cell. For the analysis of stimulus selectivity, we included every neuron for which we presented at least five repetitions of at least four different stimuli. Average firing rates were extracted from a 150-ms window starting 50 ms after stimulus onset. Neurons that never fired a spike in response to one of the test stimuli were excluded ($n = 5$), as most of our selectivity measures are ill defined under these conditions and we cannot be certain that the cells were visual in nature.

Stimulus selectivity was calculated with a variety of measures that have been previously used in visual neurophysiology studies: depth of selectivity (DOS; Moody et al. 1998; Rainer and Miller 2000), breadth of selectivity (Freedman et al. 2006), selectivity index (SI), and broadness.

$$DOS = [n - (\sum R_i/R_{max})]/[n - 1]$$

where $n$ is the number of stimuli presented, $R_i$ is the firing rate of the neuron to the presentation of the $i$th stimulus, and $R_{max}$ is the largest firing rate across all presented images.

$$breadth = 1 - median(R_{norm})$$

where $R_{norm}$ is the normalized firing rates on a scale from 0 (response to the least effective image, $R_{min}$) to 1 (response to the most effective image, $R_{max}$). DOS and breadth account for the response of the cell to all presented stimuli and range from 0 to 1, with higher values indicating more selective tuning (i.e., fewer stimuli strongly activate the cell).

$$SI = (R_{max} - R_{min})/(R_{max} + R_{min})$$

where $R_{max}$ and $R_{min}$ are the mean firing rates to the most and least effective stimuli, respectively. This value ranges from 0 to 1, with higher values indicating more selective tuning.

Broadness was defined as the proportion of stimuli eliciting a significant response from the cell. Broadness ranges from 0 to 1, with lower values indicating more selective tuning. Two related measures were calculated with different criteria for defining a significant response. First, $broadness_{wilcoxon}$ was defined as the proportion of stimuli that induced a response greater than the spontaneous firing rate of the cell (i.e., positive response or stimulus-evoked excitation) as indicated by a Wilcoxon rank-sum test ($\alpha = 0.01$). Second, $broadness_{\%max}$ was defined as the proportion of stimuli that induced responses >25% of the baseline-to-peak difference ($R_{max}$ − spontaneous rate).

Response latencies for each cell were calculated with two distinct metrics. Both metrics account for the background firing rate of the cell, and thus are little affected by differences in mean firing rate across the two cell types. First, we estimated spike density functions (SDFs) for each neuron across all screening task trials containing stimuli that elicited a significant response as defined by $broadness_{\%max}$ (see above). We used the more liberal of the two broadness measures to maximize the data included in subsequent analyses. We computed SDFs by replacing each spike with an asymmetric function composed of separate truncated Gaussian functions, one for the prespike time range (standard deviation of 5 ms) and one for the postspike time range (standard deviation of 15 ms). The asymmetric function provides an estimate of the instantaneous firing rate while minimizing the influence of each spike on the SDF backward in time (Brincat and Connor 2004; Thompson et al. 1996). Onset latency ($Lat_{SDF}$) was defined as the time that the SDF exceeded 10% of the baseline-to-peak difference and continued to increase for at least 15 ms. This second criterion was adjusted for some cells ($n = 28$) upon visual inspection of the stimulus-evoked SDF to account for responses that were either very brief (e.g., cells with consistent transient SDF increases spanning <15 ms) or very noisy (e.g., cells with low background rates that were susceptible to SDF increases driven by very few spikes that were inconsistent across stimulus repetition). Twenty-eight neurons were excluded from this analysis because the associated SDF had no clear peak ($n = 9$) or had a maximum value of <10 spikes/s (i.e., essentially just noise, $n = 19$).

The second latency metric was based on identifying "bursts," defined as times when the number of observed spikes exceeded the number expected from a Poisson process with the same mean firing rate as the cell (Hanes et al. 1995; Legendy and Salcman 1985; Sheinberg and Logothetis 2001). Mean firing rates were calculated across all recorded spikes because of the extremely low firing rates of some cells. The burst detection algorithm is described in detail by Sheinberg and Logothetis (2001). Burst onsets and offsets were defined as the time of the first and last spike of each identified burst. For each neuron, burst latency ($Lat_{burst}$) was defined as the median burst onset time across all trials in which a burst onset occurred between 40 and 200 ms after stimulus onset.

In addition to the cell-specific latency metrics described above, we calculated population response profiles for each cell type by extracting the stimulus-evoked response of each neuron to the presentation of any stimulus that elicited a significant response, as defined by $broadness_{\%max}$ (see above). Activity was normalized for each neuron, with 0 being the background firing rate and 1 being the response to the most effective image. Significant differences between putative inhibitory and putative excitatory neurons were determined by a permutation test. We calculated the difference between the normalized population averages across cell type after randomly assigning the putative

inhibitory and putative excitatory labels 5,000 times and compared the observed difference to the permutated differences at every time point. Observed differences that exceeded the 95% confidence interval of the permutated distribution for a minimum of 5 consecutive time bins were deemed significant (i.e., 2-tailed test with an $\alpha$-level of 0.05).

To explore the functional response properties of putative inhibitory and putative excitatory neurons during more natural conditions, we calculated similar selectivity and latency metrics as described above for the sudden-onset condition while the monkeys performed a self-guided visual search. For these analyses, we extracted saccade- and fixation-triggered averages of neural activity. We collapsed across all saccade directions because of the large, bilateral receptive fields of inferior temporal cortex neurons (Gross et al. 1969, 1972; Op De Beeck and Vogels 2000) and the success of this method in previous studies (Mruczek and Sheinberg 2007a, 2007b; Rolls et al. 2003; Sheinberg and Logothetis 2001). We excluded the very first saccade or fixation of each trial in order to verify that any observed effects were not driven by the initial transient response to the stimulus onset, which was quantified in the analysis of the screening trial data described above. Additionally, we excluded saccades $<1.5°$ of visual angle in amplitude or fixations that were located on the same object as the preceding fixation. These restrictions eliminated microsaccades and corrective fixations.

To quantify stimulus selectivity during visual search, we extracted fixation-triggered responses from a 125-ms window starting 50 ms after fixation onset. Where applicable, we compared this activity with a measure of baseline activity extracted from a 50-ms window centered on the fixation onset. We included every neuron for which we could extract a minimum of five fixations of at least four different stimuli. For each cell, we calculated DOS, breadth, SI, $\text{broadness}_{\text{wilcoxon}}$, and $\text{broadness}_{\%\text{max}}$ as defined above.

To quantify response latency during visual search, we extracted fixation-triggered responses for every fixation of a stimulus that elicited a significant response during the screening task, as defined by $\text{broadness}_{\%\text{max}}$ (see above). $\text{Lat}_{\text{SDF}}$ was defined as the time that the SDF exceeded 10% of the minimum-to-maximum SDF range between 25 and 175 ms after fixation onset and continued to increase for at least 15 ms. This second criterion was adjusted for some cells ($n$ = 14) upon visual inspection of the stimulus-evoked SDF to account for responses that were either very brief or very noisy. We calculated onset latency for every neuron for which we could extract a minimum of five fixations of an effective stimulus. Five neurons were excluded from this analysis because the associated SDF had no clear peak ($n$ = 2) or had a maximum value of $<10$ spikes/s (i.e., essentially just noise, $n$ = 3). $\text{Lat}_{\text{burst}}$ was defined as the median burst onset time across all fixations in which a burst onset occurred between 25 and 175 ms after fixation onset.

As with the sudden-onset analysis, we calculated population response profiles for each cell type by extracting the response of each neuron aligned to every saccade toward or fixation of a stimulus that elicited a significant response during the screening task, as defined by $\text{broadness}_{\text{wilcoxon}}$ (see above). Activity was normalized based on the response of each neuron during the screening task, with 0 being the background firing rate and 1 being the response to the most effective image. For each cell and event type, normalized activity was averaged across all neurons for which we could extract at least five saccade or fixation events. Significant differences between putative inhibitory and putative excitatory neurons were calculated with a permutation test as described for the analysis of the screening task data above.

Selectivity and latency metrics were directly compared across the sudden-onset conditions of the screening task and the fixation-aligned conditions of the visual search task. This analysis included only those neurons for which valid measures could be determined under both conditions. Significant differences across condition were determined with a Wilcoxon signed-rank test.

The distributions of the cell-specific measures were compared across putative inhibitory and putative excitatory neurons with a Wilcoxon rank sum test. Median values for each measure are reported unless otherwise specified. All statistical analyses were performed with MATLAB (MathWorks, Natick, MA) and custom software. Unless otherwise noted, significance was determined with an $\alpha$-level of 0.05.

## RESULTS

*Cell classification by waveform properties.* We recorded from 322 inferior temporal cortex neurons in 4 monkeys (42 from *monkey M*, 97 from *monkey S*, 111 from *monkey Q*, and 72 from *monkey V*). Neurons were classified as putative inhibitory or putative excitatory with two independent methods based on properties of the average spike waveform. First, spike duration was defined as the time from the initial peak to the trough (Fig. 1*A*, *inset*; Bartho et al. 2004; Mitchell et al. 2007). The distribution of spike durations for the entire population is shown in Fig. 1*A*. Hartigan's dip test (Hartigan and Hartigan 1985) confirmed that this distribution departed from unimodality ($P$ = 0.004, permutation test). We modeled this distribution by a sum of two Gaussian distributions and used the local minimum (352 $\mu$s) of the combined distribution as the cutoff for classification. Neurons with waveform durations below the cutoff threshold were defined as putative inhibitory neurons ($n$ = 70; 21.7%), and those with waveform durations greater than the threshold were classified as putative excitatory neurons ($n$ = 252; 78.3%).

We confirmed this classification with an independent $k$-means clustering procedure using the peak amplitude-normal-

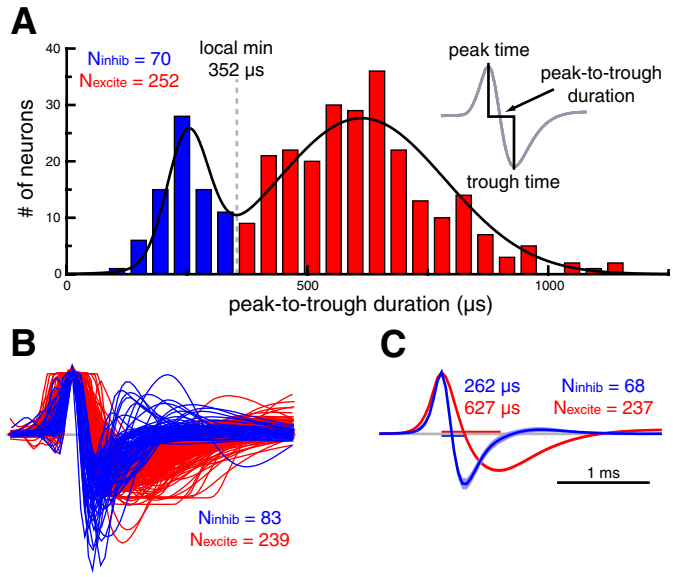


Fig. 1. Spike waveform-based classification of inferior temporal cortex neurons as putative inhibitory or putative excitatory. *A*: histogram of peak-to-trough waveform durations (*inset*) for the population of inferior temporal cortex neurons. We fit this distribution with a sum of 2 Gaussians (black trace) and used the local minimum (352 $\mu$s) as the cutoff for our waveform duration-based classification. Throughout all figures, data pertaining to putative excitatory and putative inhibitory neurons are shown in red and blue, respectively. *B*: amplitude-normalized waveform vectors sorted by a $k$-means clustering algorithm. The cluster with shorter waveform durations was deemed putative inhibitory. Timescale is the same as in *C*. *C*: average waveform for putative inhibitory and putative excitatory neurons that were consistently classified by the waveform duration-based and $k$-means clustering algorithms. Median waveform durations are shown for both distributions. Shaded region denotes 95% confidence interval.

ized waveform vectors. Figure 1*B* shows the results of this clustering analysis. The cluster with the shorter waveform durations was deemed putative inhibitory ($n = 83$; 25.8%) and the other cluster putative excitatory ($n = 239$; 74.2%). It is clear that spike duration was a critical component of the clustering algorithm. Indeed, only 17 neurons (5.3%) were classified differently by the two methods.

For the remaining analyses we have only included those neurons ($n = 305$, $N_{excite} = 237$, $N_{inhib} = 68$) that were consistently classified by both methods. Qualitatively similar results were obtained when using each classification method independently. Inconsistently classified neurons are considered separately below.

Figure 1*C* shows the average waveform for putative inhibitory and putative excitatory neurons that were consistently classified by the waveform- and cluster-based methods. The median waveform durations for putative inhibitory and putative excitatory neurons were 262 and 627 $\mu$s, respectively. In addition to longer spike durations, putative excitatory neurons had significantly lower trough amplitudes relative to their peak amplitude ($amp\_ratio_{excite} = 0.61$, $amp\_ratio_{inhib} = 0.86$, $P < 0.001$). These waveform signatures are a result of a slower repolarization phase for excitatory neurons and are consistent with both extracellular (Mitchell et al. 2007) and intracellular (McCormick et al. 1985) studies.

*Validation of classification.* To validate our classification, we measured response properties of each neuron that are known to differ across inhibitory and excitatory neurons from intracellular recordings (Connors and Gutnick 1990; Contreras and Palmer 2003; McCormick et al. 1985). First, putative inhibitory neurons from our population had higher spontaneous firing rates (4.6 spikes/s) than putative excitatory neurons (2.1 spikes/s, $P < 0.001$; Fig. 2*A*). Second, putative inhibitory neurons had higher stimulus-evoked firing rates in response to their most effective stimulus (30.4 spikes/s) than putative excitatory neurons (24.0 spikes/s, $P = 0.025$; Fig. 2*B*).

In contrast to fast-spiking inhibitory neurons, regular-spiking excitatory neurons show marked spike rate adaptation in response to prolonged current injections (Connors and Gutnick 1990; McCormick et al. 1985). These differences presumably reflect the biophysical properties of the specific ion channels expressed by each of these cell types (Martina and Jonas 1997; Martina et al. 1998; McBain and Fisahn 2001). Because we could not control the amount of stimulus-driven input to our recorded cells, we quantified the degree to which spike waveform properties (e.g., trough amplitude) adapted for spikes that occurred within very close succession (Fig. 2*C*). We reasoned that the same ion channel properties responsible for spike rate fatigue in excitatory neurons might lead to observable changes in spike waveform properties. Indeed, changes in spike waveform amplitude and duration, as a function of interspike interval, have been reported previously (Fee et al. 1996; McCormick et al. 1985).

For each neuron, we identified spike pairs that occurred within 8 ms of each other, after a preceding period of at least 50 ms with no spikes. For all neurons with at least five such spike pairs ($n = 222$, $N_{excite} = 171$, $N_{inhib} = 51$), we compared the trough amplitude of the average first spike and the average second spike with an adaptation index (see MATERIALS AND METHODS). Positive values indicate decreased trough amplitudes for the second spike of a short interspike interval pair. Consistent with results from intracellular recordings (Connors and Gutnick 1990; McCormick et al. 1985), adaptation indexes for putative excitatory neurons (0.06) were significantly higher than for putative inhibitory neurons (0.005; $P < 0.001$), indicating more pronounced waveform changes following very short interspike intervals (Fig. 2*D*). Similar results were found for other waveform parameters, such as peak-to-trough slope ($AI_{slope\_excite} = 0.05$, $AI_{slope\_inhib} = 0.009$; $P < 0.001$) and peak-to-trough duration ($AI_{dur\_excite} = -0.05$, $AI_{dur\_inhib} = 0.00$; $P = 0.001$). It should be noted that across all cells the changes in waveform duration observed here for short interspike interval spike pairs were close to an order of magnitude smaller (~41 $\mu$s) than the overall difference between putative inhibitory and putative excitatory neurons (~365 $\mu$s).

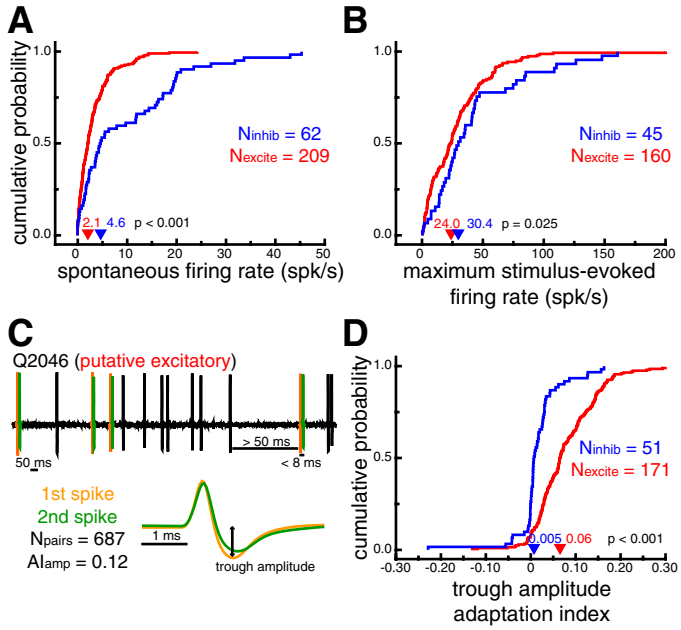


Fig. 2. Verification of neuron classification based on known response properties. *A*: cumulative probability distributions of spontaneous firing rates. Putative inhibitory neurons had larger spontaneous firing rates ($P < 0.001$). *B*: cumulative probability distributions of stimulus-evoked firing rates in response to the most effective stimulus for each cell. Putative inhibitory neurons had larger stimulus-evoked firing rates ($P = 0.025$). *C*: illustration of the waveform adaptation analysis for a sample time window of an example putative excitatory neuron. Spike pairs that occurred within 8 ms of each other, after a preceding period of at least 50 ms with no spikes, were extracted from the stored extracellular trace (*top*). Average waveforms for the first (orange) and second (green) spike of each pair were compared with an adaptation index (AI). *D*: cumulative probability distributions of trough amplitude adaptation indexes. Positive values indicate decreased trough amplitudes for the second spike of a short interspike interval pair. Putative excitatory neurons displayed more pronounced waveform adaptation as measured by changes in trough amplitude ($P < 0.001$). In *A*, *B*, and *D*, arrowheads denote median values.

*Stimulus selectivity.* The neural response to each image was extracted from a 150-ms window starting 50 ms after stimulus onset during the screening task. Figure 3*A* shows the normalized neural response, ranked by stimulus effectiveness, for all neurons recorded during the presentation of at least five repetitions of four images ($n = 167$, $N_{excite} = 132$, $N_{inhib} = 35$). Because of the nature of our screening task, the number of images meeting these criteria differed across cell. Overall, however, the number of images included in this analysis did not differ across neuron type (median: $N_{excite} = 12$, $N_{inhib} =$

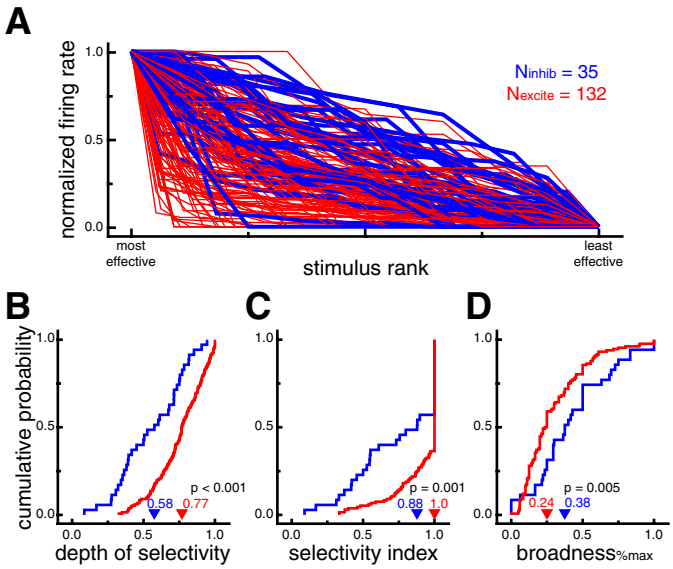


Fig. 3. Putative excitatory neurons exhibit stronger stimulus selectivity than putative inhibitory neurons during sudden-onset presentation. *A*: normalized neural responses for each cell ranked by stimulus effectiveness. Putative excitatory neurons generally showed stronger stimulus selectivity as indicated by the relatively sharper drop-off in normalized response across stimulus rank (i.e., more red at *bottom left* and more blue at *top right*). Putative inhibitory neuron lines are displayed thicker for ease of viewing. *B*: cumulative probability distributions of depth of selectivity (DOS). Higher values indicate more selective tuning. Putative excitatory neurons had larger DOS values, indicating stronger selectivity ($P < 0.001$). *C*: cumulative probability distributions of the stimulus selectivity index (SI). Higher values indicate more selective tuning. Putative excitatory neurons had larger SI values, indicating stronger selectivity ($P = 0.001$). *D*: cumulative probability distributions of broadness$_{\%max}$ (proportion of stimuli eliciting a response at least 25% of the maximum response). A lower proportion of stimuli evoked a significant response from putative excitatory neurons, indicating stronger selectivity ($P = 0.005$). In *B–D*, arrowheads denote median values.

12, $P = 0.87$; range$_{excite}$ = 4–35, range$_{inhib}$ = 4–20). Although there was a large overlap in the response profiles for putative inhibitory and putative excitatory neurons, putative excitatory neurons generally showed stronger stimulus selectivity as indicated by the relatively sharper drop-off in normalized response across stimulus rank.

To quantify this difference, we used a variety of selectivity measures (see MATERIALS AND METHODS). Across the population of neurons, putative excitatory neurons displayed significantly higher values for depth of selectivity (DOS$_{excite}$ = 0.77, DOS$_{inhib}$ = 0.58, $P < 0.001$; Fig. 3*B*), breadth (breadth$_{excite}$ = 0.83, breadth$_{inhib}$ = 0.67, $P < 0.001$), and selectivity index (SI$_{excite}$ = 1.0, SI$_{inhib}$ = 0.88, $P = 0.001$; Fig. 3*C*). The selectivity index was also significant (SI$_{excite}$ = 0.79, SI$_{inhib}$ = 0.55, $P = 0.0007$) when excluding all cells with SI of 1.0, which occurs when a cell does not fire any spikes in response to at least one stimulus. There was no significant difference between broadness$_{wilcoxon}$ values, in which significant responses were defined by a Wilcoxon rank sum test (broadness$_{wilcoxon_excite}$ = 0.20, broadness$_{wilcoxon_inhib}$ = 0.21, $P = 0.99$). However, an alternative quantification of stimulus-evoked responses (% of maximum response, see MATERIALS AND METHODS) yielded results consistent with DOS, breadth, and selectivity indexes, with significantly lower values of broadness$_{\%max}$ for putative excitatory than putative inhibitory neurons (broadness$_{\%max_excite}$ = 0.24, broadness$_{\%max_inhib}$ = 0.38 $P = 0.005$; Fig. 3*D*). Overall, these results indicate that putative inhibitory neurons displayed stimulus-evoked responses across a larger proportion of images than putative excitatory neurons.

*Response latency.* Figure 4*A* shows the population-averaged neuronal response during the screening task to a subset of images evoking a significant response, sorted by cell type. From this plot, it appears that putative inhibitory neurons responded slightly earlier than putative excitatory neurons. Indeed, the difference between the response functions of the two cell classes was significant for the population-averaged traces starting 81 ms after stimulus onset ($P < 0.05$, permutation test). To quantify this latency difference more directly, we estimated response latencies for each of our neurons, using two distinct metrics based on either the SDF or a Poisson spiking model. Figure 4*B* shows the estimated response latencies using both metrics for example putative excitatory and putative inhibitory neurons.

First, SDFs for each neuron were estimated from all stimuli that elicited a significant response, as defined by the broadness$_{\%max}$ metric. Lat$_{SDF}$ was defined as the time that the SDF exceeded 10% of the baseline-to-peak difference. This

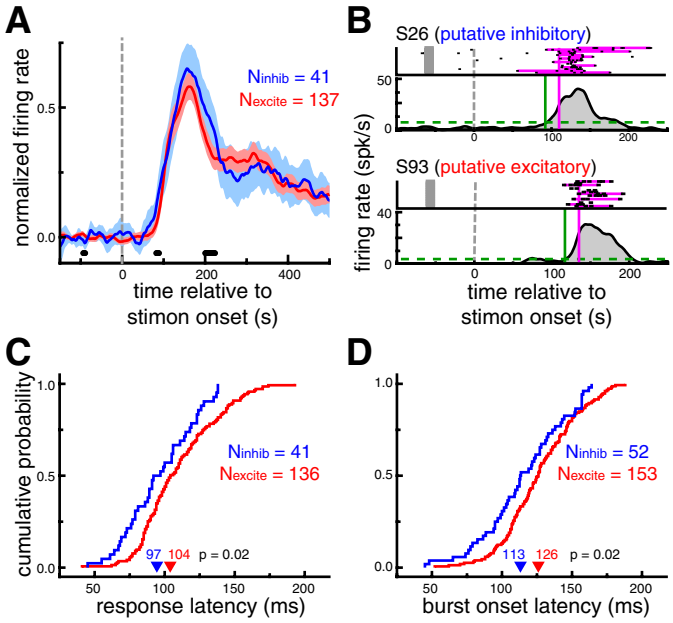


Fig. 4. Putative inhibitory neurons exhibit shorter response latencies than putative excitatory neurons during sudden-onset presentation. *A*: population-averaged neuronal response to a subset of images evoking a significant response. Shaded region denotes 95% confidence interval. Thick black marks denote time points at which the difference between 2 cell types was significant ($P < 0.05$, permutation test). Putative inhibitory neurons responded slightly earlier than putative excitatory neurons; the population-averaged response function for putative inhibitory neurons was significantly higher than putative excitatory neurons in the 81–89 ms range ($P < 0.05$). *B*: response latency estimation for examples of an putative inhibitory (*top*) and a putative excitatory (*bottom*) neuron. Response latencies were estimated with 2 distinct metrics. Response onset latency (Lat$_{SDF}$, green) was defined as the time that the spike density function (SDF) exceeded 10% of the baseline-to-peak difference (dashed line). Burst latency (Lat$_{burst}$, pink) was defined as the median time that the spike train first departed from a Poisson spiking process with the same mean firing rate as the neuron. Spikes comprising bursts are highlighted in pink. Note that only a small selection of trials is displayed in the raster plot for each neuron. *C*: cumulative probability distributions of response onset latencies (Lat$_{SDF}$). Putative inhibitory neurons had shorter response onset latencies ($P = 0.02$). *D*: cumulative probability distributions of burst onset latencies (Lat$_{burst}$). Putative inhibitory neurons had shorter burst onset latencies ($P = 0.02$). In *C* and *D*, arrowheads denote median values.

metric was only computed for neurons with at least one image that evoked a significant response and a peak SDF value of at least 10 spikes/s ($N_{excite}$ = 136, $N_{inhib}$ = 41). Across this population of neurons, putative inhibitory neurons displayed significantly shorter response onset latencies (97 ms) than putative excitatory neurons (104 ms, $P$ = 0.02; Fig. 4*C*).

The second latency measure was based on identifying spike "bursts." Bursts were defined as spike trains that departed from a Poisson spiking process with the same mean firing rate as the cell. $Lat_{burst}$ was defined as the median time of the first spike in identified bursts across all trials. Note that, unlike $Lat_{SDF}$, this measure was not dependent on first identifying a subset of trials in which a specific image was presented. Across the population of neurons exhibiting bursts ($N_{excite}$ = 153; $N_{inhib}$ = 52), putative inhibitory neurons displayed significantly shorter burst latencies (113 ms) than putative excitatory neurons (126 ms, $P$ = 0.02; Fig. 4*D*).

*Natural viewing conditions.* To determine how the stimulus selectivity and response latency differences observed for putative excitatory and putative inhibitory neurons were affected by more natural viewing conditions, we calculated metrics similar to those described above for the sudden-onset condition of the screening task while the monkeys performed a self-guided visual search task. The majority of these analyses were based on the neural response elicited for each fixation, excluding the very first fixation of every search trial.

Figure 5*A* shows the normalized neural response, ranked by stimulus effectiveness, for all neurons recorded while the monkey made a minimum of five fixations of four different images during the visual search task ($n$ = 209, $N_{excite}$ = 169, $N_{inhib}$ = 40). Neural responses were calculated from a 125-ms window starting 50 ms after fixation onset during visual search trials. Putative excitatory neurons generally showed stronger stimulus selectivity as indicated by the relatively sharper drop-off in normalized response across stimulus rank. Consistent with the results from the sudden-onset analysis of the screening task, putative excitatory neurons displayed significantly higher values for depth of selectivity ($DOS_{excite}$ = 0.71, $DOS_{inhib}$ = 0.45, $P < 0.001$; Fig. 5*B*), breadth ($breadth_{excite}$ = 0.77, $breadth_{inhib}$ = 0.63, $P < 0.001$), and selectivity index ($SI_{excite}$ = 1.0, $SI_{inhib}$ = 0.61, $P < 0.001$; Fig. 5*C*) and significantly lower values of broadness$_{\%max}$ ($broadness_{\%max\_excite}$ = 0.20, $broadness_{\%max\_inhib}$ = 0.30, $P < 0.001$; Fig. 5*D*) during self-guided visual search. The selectivity index was also significant ($SI_{excite}$ = 0.81, $SI_{inhib}$ = 0.48, $P < 0.001$) when excluding all cells with SI of 1.0, which occurs when a cell does not fire any spikes during fixation of at least one stimulus.

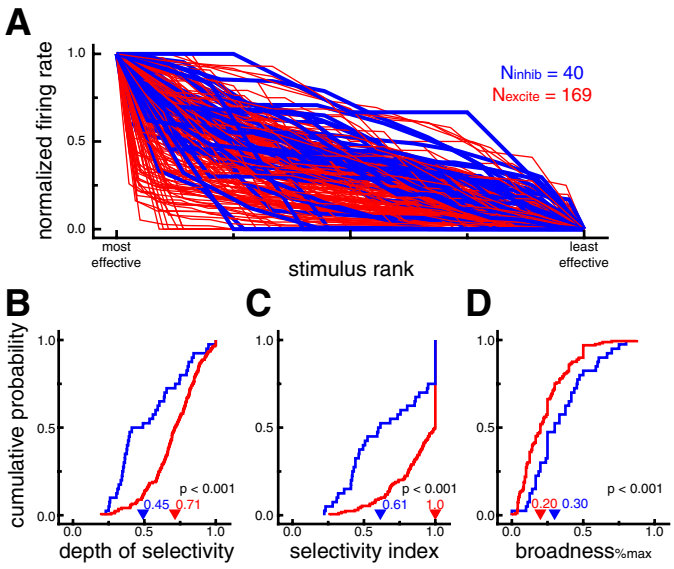


Fig. 5. Putative excitatory neurons exhibit stronger stimulus selectivity than putative inhibitory neurons during self-guided visual search. *A*: normalized fixation-triggered neural responses for each cell ranked by stimulus effectiveness. Putative excitatory neurons generally showed stronger stimulus selectivity as indicated by the relatively sharper drop-off in normalized response across stimulus rank (i.e., more red at *bottom left* and more blue at *top right*). Putative inhibitory neuron lines are displayed thicker for ease of viewing. *B*: cumulative probability distributions of DOS. Higher values indicate more selective tuning. Putative excitatory neurons had larger DOS values, indicating stronger selectivity ($P < 0.001$). *C*: cumulative probability distributions of SI. Higher values indicate more selective tuning. Putative excitatory neurons had larger SI values, indicating stronger selectivity ($P < 0.001$). *D*: cumulative probability distributions of broadness$_{\%max}$. A lower proportion of stimuli evoked a significant response from putative excitatory neurons, indicating stronger selectivity ($P < 0.001$). In *B–D*, arrowheads denote median values.

We directly compared stimulus selectivity across the sudden-onset conditions of the screening task and the fixation-aligned conditions of the visual search task for all putative inhibitory ($n$ = 24) and putative excitatory ($n$ = 106) neurons for which we could calculate valid metrics for each condition. In general, putative inhibitory neurons showed no difference in selectivity across condition ($DOS_{onset}$ = 0.61, $DOS_{search}$ = 0.59, $P$ = 0.95; $breadth_{onset}$ = 0.71, $breadth_{inhib\_search}$ = 0.64, $P$ = 0.76; $SI_{onset}$ = 0.77, $SI_{search}$ = 0.75, $P$ = 0.62). Putative excitatory neurons, on the other hand, showed small but significant decreases in selectivity during visual search ($DOS_{onset}$ = 0.78, $DOS_{search}$ = 0.72, $P < 0.001$; $breadth_{onset}$ = 0.85, $breadth_{excite\_search}$ = 0.77, $P$ = 0.001; $SI_{onset}$ = 1.0, $SI_{search}$ = 0.96, $P$ = 0.01). These results are consistent with previous work showing that most inferior temporal cortex neurons exhibit similar degrees of stimulus selectivity when objects are viewed in isolation or fixated during visual search (Sheinberg and Logothetis 2001).

To show the population response dynamics during visual search, we calculated saccade (Fig. 6*A*)- and fixation (Fig. 6*B*)-triggered averages of neural activity for each cell type. This analysis included saccades toward or fixations of any stimulus that elicited a significant response during the screening task, as defined by broadness$_{\%max}$. For neurons recorded during at least five such events of either type ($N_{sac\_excite}$ = 64, $N_{sac\_inhib}$ = 11; $N_{fix\_excite}$ = 69, $N_{fix\_inhib}$ = 13), mean normalized activity traces were directly compared across cell type with a permutation test. Putative inhibitory neurons showed response modulations that were significantly greater than putative excitatory neurons as early as 89 ms after a saccade onset and 50 ms after fixation onset. For comparison, in the sudden-onset analysis described above, differences between the two cell classes emerged 81 ms after stimulus onset.

Significant differences across cell type were also apparent prior to saccades toward or fixations of an effective stimulus during visual search. These differences presumably reflect the broader selectivity of putative inhibitory neurons (Fig. 5), as the identity of the object fixated prior to the analyzed event was not specifically selected. Importantly, no significant differences were apparent at the time of the saccade or at the beginning of the fixation, and thus differences do not simply reflect higher activity for putative inhibitory neurons throughout visual search conditions. Addition-

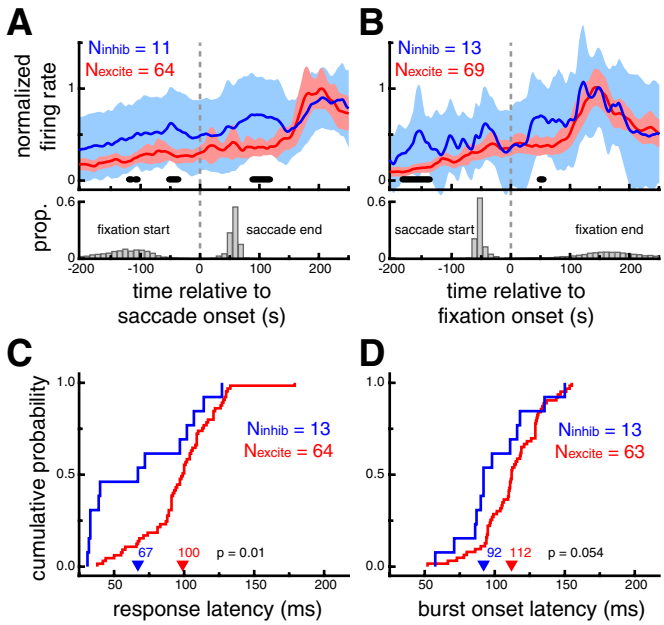


Fig. 6. Putative inhibitory neurons exhibit shorter response latencies than putative excitatory neurons during self-guided visual search. *A*: saccade-triggered neural response averages during the search task for saccades that landed on an image that elicited a significant response during the screening trials (*top*) and the distributions of the saccade end time and the previous fixation start time (*bottom*). *B*: fixation-triggered neural response averages during the search task for fixation that were located on an image that elicited a significant response during the visual search task (*top*) and the distributions of the fixation end time and the previous saccade start time. For *A* and *B*, shaded region denotes 95% confidence interval and thick black marks denote time points at which the difference between the 2 cell types was significant ($P < 0.05$, permutation test). Putative inhibitory neurons showed earlier modulations, ~89 ms after saccade onset and as early as 50 ms after fixation onset. Importantly, no significant differences were apparent at the time of the saccade or at the beginning of the fixation. *C*: cumulative probability distributions of response onset latencies ($Lat_{SDF}$). Putative inhibitory neurons had shorter response onset latencies ($P = 0.01$). *D*: cumulative probability distributions of burst onset latencies ($Lat_{burst}$). Putative inhibitory neurons had marginally shorter burst onset latencies ($P = 0.054$). In *C* and *D*, arrowheads denote median values.

ally, we did not observe any difference in the saccade- or fixation-aligned neural response profiles in the absence of visual stimuli (i.e., intertrial intervals, data not shown).

For a more direct comparison with the sudden-onset conditions of the screening task, we estimated fixation-triggered response latencies during visual search, using the same metrics. $Lat_{SDF}$ was defined as the time that the SDF exceeded 10% of the minimum-to-maximum range after fixation onset and was computed for all neurons recorded during the fixation of at least five stimuli that evoked a significant response during the screening task. Across this population of neurons ($N_{excite} = 64$, $N_{inhib} = 13$), putative inhibitory neurons displayed significantly shorter fixation-aligned response onset latencies (67 ms) than putative excitatory neuron (100 ms, $P = 0.01$; Fig. 6*C*). $Lat_{burst}$ was defined as the median time of the first spike in identified bursts (see above) across all fixations during the visual search. Across the population of neurons exhibiting bursts ($N_{excite} = 63$, $N_{inhib} = 13$), putative inhibitory neurons displayed shorter burst latencies (92 ms) than putative excitatory neurons (112 ms), although this difference was only marginally significant ($P = 0.054$; Fig. 6*D*).

We directly compared response latencies derived from the sudden-onset condition of the screening task and the fixation-aligned condition of the visual search task for all neurons for which we could calculate valid onset ($N_{excite} = 65$, $N_{inhib} = 13$) and burst ($N_{excite} = 62$, $N_{inhib} = 13$) latencies for each condition. Putative inhibitory neurons had significantly faster response latencies during visual search ($Lat_{SDF\_onset} = 91$ ms, $Lat_{SDF\_search} = 67$ ms, $P = 0.02$; $Lat_{burst\_onset} = 113$ ms, $Lat_{burst\_search} = 92$ ms, $P = 0.04$). Putative excitatory neurons showed no effect of condition on response latency ($Lat_{SDF\_onset} = 95$ ms, $Lat_{SDF\_search} = 99$ ms, $P = 0.94$; $Lat_{burst\_onset} = 114$ ms, $Lat_{burst\_search} = 112$ ms, $P = 0.52$).

In summary, during self-guided search through complex visual displays, the relationship between the selectivity of putative inhibitory and putative excitatory neurons was similar to sudden-onset conditions, with putative excitatory neurons responding to a more narrow range of images. Additionally, the response latency differences between putative inhibitory and putative excitatory neurons were enhanced compared with those measured under sudden-onset conditions.

*Inconsistently classified neurons.* The above analyses were limited to those neurons that were consistently classified as putative inhibitory or putative excitatory by both the waveform duration and clustering methods. Here, we briefly provide some more details about the subset of neurons ($n = 17$) that were inconsistently classified across the two methods. In general, these neurons displayed spike waveform properties that were distinct from both putative excitatory and putative inhibitory neurons and functional properties that were more similar to those of putative excitatory neurons.

Specifically, the neurons that were inconsistently classified tended to have spike waveform durations (378 $\mu$s) just above the waveform-based classification cutoff value of 352 $\mu$s. Similar to putative excitatory neurons, inconsistently classified cells showed significantly more spike waveform adaptation during very short interspike intervals than putative inhibitory neurons ($AI_{amp\_inconsistent} = 0.067$, $P = 0.009$). Similar to putative inhibitory neurons, however, they had significantly higher trough amplitudes relative to their waveform peak amplitude than putative excitatory neurons ($amp\_ratio_{inconsistent} = 0.87$, $P = 0.003$). It is possible that these neurons represent an additional and distinct class of cells, such as "chattering cells" (Gray and McCormick 1996; Mitchell et al. 2007; Nowak et al. 2003) or a class of long-range projection neurons (Vigneswaran et al. 2011). Consistent with this hypothesis, the functional properties of these neurons were more similar to those of putative excitatory neurons. The inconsistently classified population showed trends toward lower spontaneous (2.4 spikes/s, $P = 0.15$) and stimulus-evoked (17.1 spikes/s, $P = 0.10$) firing rates, as well as higher stimulus selectivity ($dos_{inconsistent} = 0.76$, $P = 0.051$; $breadth_{inconsistent} = 0.88$, $P = 0.003$) compared with putative inhibitory neurons. No significant differences were found between inconsistently classified cells and putative excitatory neurons for the same measures ($P > 0.52$ in all cases).

## DISCUSSION

We classified inferior temporal cortex neurons as putative excitatory or putative inhibitory on the basis of their extra-

cellular waveform properties. As expected, putative inhibitory neurons had larger spontaneous and stimulus-driven firing rates than putative excitatory neurons. Additionally, putative excitatory neurons displayed more pronounced spike waveform adaptation following very short interspike intervals. Finally, we compared two functional properties of each neuron's stimulus-evoked response: stimulus selectivity and response latency. Across a range of measures, putative excitatory neurons showed stronger stimulus selectivity compared with putative inhibitory neurons. Putative inhibitory neurons, on the other hand, showed shorter response latencies compared with putative excitatory neurons. Furthermore, differences in stimulus selectivity were maintained and differences in response latency were enhanced during a visual search task emulating more natural viewing conditions: a cluttered environment, self-guided exploration, and goal-oriented behavior.

*Comparison with previous results.* Our population contained ~22% putative inhibitory neurons, which is consistent with previous reports from histological studies (~25%; Hendry et al. 1987). One might expect that our population should comprise a higher proportion of pyramidal cells because of the sampling bias of the extracellular recording technique (Logothetis 2003; Towe and Harding 1970). However, in our case this sampling bias may be counteracted, at least partially, because of the extremely low spontaneous firing rate of many inferior temporal cortex neurons (Fig. 2*A*). It is likely that many excitatory pyramidal cells were not recorded simply because we were unaware of their proximity to the electrode tip in the absence of an effective visual image.

Tamura et al. (2004) compared excitatory and inhibitory inferior temporal cortex neurons identified with paired recordings and a cross-correlation analysis. Quantifying selectivity with a broadness metric (same as $\text{broadness}_{\text{wilcoxon}}$ here), they did not find any difference between inhibitory and excitatory neurons. Although we found similar results for $\text{broadness}_{\text{wilcoxon}}$, we also found highly significant differences using selectivity metrics that were more sensitive to the entire range of evoked responses (DOS and breadth) and an alternative definition for significant stimulus-evoked activity ($\text{broadness}_{\%\text{max}}$). Finally, consistent with our results, a plot of the average time course of the response to the most effective stimulus (their Fig. 6) shows a relatively earlier response onset for putative inhibitory neurons, although the authors did not quantify this effect.

Zoccolan et al. (2007) classified inferior temporal cortex neurons on the basis of their extracellular waveform and noted a tendency for putative inhibitory neurons to show weaker stimulus selectivity (DOS and sparseness; Olshausen and Field 2004; Rolls and Tovee 1995) than putative excitatory neurons. Interestingly, they also noted that putative inhibitory neurons were more tolerant to changes in spatial position, size, contrast, and clutter (i.e., flanking stimuli). In other words, putative inhibitory neurons responded to a larger proportion of stimuli and over a larger range of identity-preserving image manipulations.

A similar relationship between response latency and stimulus selectivity as shown here, but without specific regard to cell type, has been shown in both monkey and human temporal cortical neurons. Sugase et al. (1999) showed that the earliest component of the response to faces in inferior temporal cortex and the superior temporal sulcus (STS) is more broadly tuned to global information (e.g., monkey vs. human), while later components carry more specific information (e.g., identity and emotional state). Similarly, Brincat and Connor (2006) showed that neurons in posterior inferior temporal cortex that are sensitive to individual stimulus parts had shorter response latencies than neurons sensitive to nonlinear combinations of multiple stimulus parts. Zoccolan et al. (2007) and Mormann et al. (2008) reported a direct relationship between response latency and stimulus selectivity in monkey inferior temporal cortex and human medial temporal cortex, respectively: neurons with shorter response latencies tended to be less selective. Interestingly, Mormann et al. (2008) also noted that the cells with shorter latencies and broader selectivity generally had high spontaneous firing rates. Our data suggest that this population may have contained a high proportion of inhibitory interneurons.

Finally, it is worth noting that our results are consistent with a wide range of studies from multiple cortical regions across multiple species. In monkeys, Diester and Nieder (2008) found higher selectivity and a later emergence of selectivity for number representations in putative excitatory prefrontal cortex neurons. Similarly, Hussar and Pasternak (2009) reported a trend for putative inhibitory neurons to show earlier task-related changes in directional selectivity. More directly, Wilson et al. (1994) found that putative inhibitory neurons responded at shorter latencies than neighboring putative excitatory neurons. Also in prefrontal cortex, Constantinidis and Goldman-Rakic (2002) found that putative inhibitory interneurons had broader spatial tuning. In parietal cortex, Yokoi and Komatsu (2010) reported that putative excitatory neurons, but not putative inhibitory neurons, showed selectivity for orientation during a visual grouping task. There was also a trend for putative excitatory parietal neurons to show longer response latencies (~10-ms difference), although this effect was not significant. In cat primary visual cortex, Cardin et al. (2007) found moderately broader orientation tuning in layer 4 inhibitory neurons and Nowak et al. (2008) found a subset of fast-spiking inhibitory neurons with little orientation or directional selectivity. Studies in mouse primary visual cortex have reported that inhibitory interneurons have larger receptive fields than excitatory neurons (Liu et al. 2009; Niell and Stryker 2008) and the large majority have much weaker orientation and spatial frequency tuning (Kerlin et al. 2010; Liu et al. 2009; Niell and Stryker 2008; Runyan et al. 2010; Sohya et al. 2007). In mouse auditory cortex, putative inhibitory interneurons exhibit less selectivity for natural stimuli, broader frequency tuning, and shorter response latencies (Lin and Liu 2010). Putative inhibitory interneurons in rat (Simons and Carvell 1989) and rabbit (Swadlow 1989) barrel (somatosensory) cortex are generally not directionally selective but are highly sensitive to vibrissa stimulation. In response to tactile stimulation, putative inhibitory neurons in rat motor cortex respond with shorter response latencies than putative excitatory neurons (Murray and Keller 2011). In the primate motor system, compared with putative regular-spiking pyramidal neurons, putative inhibitory neurons display broader directional tuning in primary motor cortex (Merchant et al. 2008) and are modulated by a wider range

of movement conditions in dorsal premotor cortex (Kaufman et al. 2010). Additionally, putative inhibitory neurons in primary motor cortex respond to movement cues with shorter response latencies compared with putative regular-spiking excitatory neurons (Merchant et al. 2008). The results from all these studies suggest a general functional distinction between inhibitory and excitatory cells across cortex that is directly supported by the present study: inhibitory neurons respond earlier and are influenced by a more diverse set of stimulus conditions than excitatory neurons.

*Mechanism and network implications.* Clarifying the differences in basic response properties between inhibitory and excitatory neurons is critically important for understanding how local cortical networks process and transform sensory information for guiding behavior. In inferior temporal cortex, inhibitory neurons contribute mainly to local circuitry (Tanigawa et al. 1998) and are known to play a role in shaping the neural response properties of excitatory neurons (Wang et al. 2000). Our latency results demonstrate that inhibitory neurons are well suited to influence excitatory neurons in that they respond earlier and to a wider variety of retinal images. Furthermore, these effects are enhanced during natural viewing conditions, when the complexity of the visual scene generates more lateral competition between cortical object representations.

Why might inhibitory neurons fire earlier? Although our data do not address this question, we can propose a few scenarios. First, inhibitory cells may simply have a lower threshold for activation (Connors and Gutnick 1990). This would also explain their higher spontaneous rates, since very little input might be needed to initiate spiking. Second, inhibitory neurons may receive preferential input from "fast" visual pathways (Chen et al. 2007). These might include, for example, direct input from the lateral geniculate nucleus (Hernandez-Gonzalez et al. 1994) or top-down inputs from prefrontal cortex representing an "initial guess" (Bar 2003), both of which would likely convey coarser, less selective, visual information. In contrast, excitatory cells may receive their dominant input via the traditional ventral visual stream hierarchy. Third, it is possible that our inhibitory population was mainly recorded from cortical input layers (e.g., layer 4) and our excitatory population mainly recorded from cortical output layers (e.g., layer 5 or 6). In this case, a local processing hierarchy could explain the latency differences. This scenario, however, is still consistent with the general hypothesis put forth above: short-latency inhibitory responses (local processing) with coarse information are well positioned to influence visual processing in excitatory (output) neurons, yielding a sparser visual representation. It should be noted that these hypotheses are not mutually exclusive. For example, in rabbit barrel cortex putative inhibitory interneurons of layer 4 receive direct input from the thalamus (Swadlow 2003).

*Conclusions.* Although the broad classification of neurons as inhibitory or excitatory is an oversimplification of the diversity of cortical cells, it is a useful step in advancing our understanding of the role these cell types play in visual processing. Our results demonstrate that, in general, putative excitatory neurons are more selective and respond with longer latencies than putative inhibitory neurons. Importantly, these functional differences were apparent during self-guided exploration through complex visual displays, suggesting that they are relevant for natural vision. Additional studies will be useful for understanding how other fundamental neuronal properties, such as receptive field structure (Op De Beeck and Vogels 2000) and experience-dependent plasticity (Anderson et al. 2008; Freedman et al. 2006; Woloszyn and Sheinberg 2012), vary across cell type. Such comparisons will be critical for developing biologically plausible models of visual processing that take into account the role of different cell types.

## ACKNOWLEDGMENTS

We thank Luke Woloszyn and Yuri Saalmann for helpful comments on the manuscript.

## GRANTS

This work was supported by the James S. McDonnell Foundation, National Eye Institute Grant R01-EY-014681, National Science Foundation Grant SBE-0542013, and the Max Planck Society.

## DISCLOSURES

No conflicts of interest, financial or otherwise, are declared by the author(s).

## AUTHOR CONTRIBUTIONS

Author contributions: R.E.M. and D.L.S. conception and design of research; R.E.M. and D.L.S. performed experiments; R.E.M. and D.L.S. analyzed data; R.E.M. and D.L.S. interpreted results of experiments; R.E.M. prepared figures; R.E.M. drafted manuscript; R.E.M. and D.L.S. edited and revised manuscript; R.E.M. and D.L.S. approved final version of manuscript.

## REFERENCES

**Anderson B, Mruczek RE, Kawasaki K, Sheinberg D.** Effects of familiarity on neural activity in monkey inferior temporal lobe. *Cereb Cortex* 18: 2540–2552, 2008.

**Bar M.** A cortical mechanism for triggering top-down facilitation in visual object recognition. *J Cogn Neurosci* 15: 600–609, 2003.

**Bartho P, Hirase H, Monconduit L, Zugaro M, Harris KD, Buzsaki G.** Characterization of neocortical principal cells and interneurons by network interactions and extracellular features. *J Neurophysiol* 92: 600–608, 2004.

**Brincat SL, Connor CE.** Dynamic shape synthesis in posterior inferotemporal cortex. *Neuron* 49: 17–24, 2006.

**Brincat SL, Connor CE.** Underlying principles of visual shape selectivity in posterior inferotemporal cortex. *Nat Neurosci* 7: 880–886, 2004.

**Cardin JA, Palmer LA, Contreras D.** Stimulus feature selectivity in excitatory and inhibitory neurons in primary visual cortex. *J Neurosci* 27: 10333–10344, 2007.

**Chen CM, Lakatos P, Shah AS, Mehta AD, Givre SJ, Javitt DC, Schroeder CE.** Functional anatomy and interaction of fast and slow visual pathways in macaque monkeys. *Cereb Cortex* 17: 1561–1569, 2007.

**Chen Y, Martinez-Conde S, Macknik SL, Bereshpolova Y, Swadlow HA, Alonso JM.** Task difficulty modulates the activity of specific neuronal populations in primary visual cortex. *Nat Neurosci* 11: 974–982, 2008.

**Connors BW, Gutnick MJ.** Intrinsic firing patterns of diverse neocortical neurons. *Trends Neurosci* 13: 99–104, 1990.

**Constantinidis C, Goldman-Rakic PS.** Correlated discharges among putative pyramidal neurons and interneurons in the primate prefrontal cortex. *J Neurophysiol* 88: 3487–3497, 2002.

**Contreras D, Palmer L.** Response to contrast of electrophysiologically defined cell classes in primary visual cortex. *J Neurosci* 23: 6936–6945, 2003.

**Csicsvari J, Hirase H, Czurko A, Mamiya A, Buzsaki G.** Oscillatory coupling of hippocampal pyramidal cells and interneurons in the behaving rat. *J Neurosci* 19: 274–287, 1999.

**Diester I, Nieder A.** Complementary contributions of prefrontal neuron classes in abstract numerical categorization. *J Neurosci* 28: 7737–7747, 2008.

**Fee MS, Mitra PP, Kleinfeld D.** Variability of extracellular spike waveforms of cortical neurons. *J Neurophysiol* 76: 3823–3833, 1996.

**Freedman DJ, Riesenhuber M, Poggio T, Miller EK.** Experience-dependent sharpening of visual shape selectivity in inferior temporal cortex. *Cereb Cortex* 16: 1631–1644, 2006.

**Gray CM, McCormick DA.** Chattering cells: superficial pyramidal neurons contributing to the generation of synchronous oscillations in the visual cortex. *Science* 274: 109–113, 1996.

**Gross CG, Bender DB, Rocha-Miranda CE.** Visual receptive fields of neurons in inferotemporal cortex of the monkey. *Science* 166: 1303–1306, 1969.

**Gross CG, Rocha-Miranda CE, Bender DB.** Visual properties of neurons in inferotemporal cortex of the macaque. *J Neurophysiol* 35: 96–111, 1972.

**Gur M, Beylin A, Snodderly DM.** Physiological properties of macaque V1 neurons are correlated with extracellular spike amplitude, duration, and polarity. *J Neurophysiol* 82: 1451–1464, 1999.

**Hanes DP, Thompson KG, Schall JD.** Relationship of presaccadic activity in frontal eye field and supplementary eye field to saccade initiation in macaque: Poisson spike train analysis. *Exp Brain Res* 103: 85–96, 1995.

**Hartigan JA, Hartigan PM.** The dip test of unimodality. *Ann Stat* 13: 70–84, 1985.

**Hendry S, Schwark H, Jones E, Yan J.** Numbers and proportions of GABA-immunoreactive neurons in different areas of monkey cerebral cortex. *J Neurosci* 7: 1503–1519, 1987.

**Henze DA, Borhegyi Z, Csicsvari J, Mamiya A, Harris KD, Buzsaki G.** Intracellular features predicted by extracellular recordings in the hippocampus in vivo. *J Neurophysiol* 84: 390–400, 2000.

**Hernandez-Gonzalez A, Cavada C, Reinoso-Suarez F.** The lateral geniculate nucleus projects to the inferior temporal cortex in the macaque monkey. *Neuroreport* 5: 2693–2696, 1994.

**Hubel DH, Wiesel TN.** Receptive fields and functional architecture of monkey striate cortex. *J Physiol* 195: 215–243, 1968.

**Hussar CR, Pasternak T.** Flexibility of sensory representations in prefrontal cortex depends on cell type. *Neuron* 64: 730–743, 2009.

**Hussar CR, Pasternak T.** Memory-guided sensory comparisons in the prefrontal cortex: contribution of putative pyramidal cells and interneurons. *J Neurosci* 32: 2747–2761, 2012.

**Johnston K, DeSouza JF, Everling S.** Monkey prefrontal cortical pyramidal and putative interneurons exhibit differential patterns of activity between prosaccade and antisaccade tasks. *J Neurosci* 29: 5516–5524, 2009.

**Kaufman MT, Churchland MM, Santhanam G, Yu BM, Afshar A, Ryu SI, Shenoy KV.** Roles of monkey premotor neuron classes in movement preparation and execution. *J Neurophysiol* 104: 799–810, 2010.

**Kerlin AM, Andermann ML, Berezovskii VK, Reid RC.** Broadly tuned response properties of diverse inhibitory neuron subtypes in mouse visual cortex. *Neuron* 67: 858–871, 2010.

**Legendy CR, Salcman M.** Bursts and recurrences of bursts in the spike trains of spontaneously active striate cortex neurons. *J Neurophysiol* 53: 926–939, 1985.

**Leopold DA, Logothetis NK.** Microsaccades differentially modulate neural activity in the striate and extrastriate visual cortex. *Exp Brain Res* 123: 341–345, 1998.

**Lin FG, Liu RC.** Subset of thin spike cortical neurons preserve the peripheral encoding of stimulus onsets. *J Neurophysiol* 104: 3588–3599, 2010.

**Liu BH, Li P, Li YT, Sun YJ, Yanagawa Y, Obata K, Zhang LI, Tao HW.** Visual receptive field structure of cortical inhibitory neurons revealed by two-photon imaging guided recording. *J Neurosci* 29: 10520–10532, 2009.

**Logothetis NK.** MR imaging in the non-human primate: studies of function and of dynamic connectivity. *Curr Opin Neurobiol* 13: 630–642, 2003.

**Markram H, Toledo-Rodriguez M, Wang Y, Gupta A, Silberberg G, Wu C.** Interneurons of the neocortical inhibitory system. *Nat Rev Neurosci* 5: 793–807, 2004.

**Martina M, Jonas P.** Functional differences in $Na^+$ channel gating between fast-spiking interneurones and principal neurones of rat hippocampus. *J Physiol* 505: 593–603, 1997.

**Martina M, Schultz JH, Ehmke H, Monyer H, Jonas P.** Functional and molecular differences between voltage-gated $K^+$ channels of fast-spiking interneurons and pyramidal neurons of rat hippocampus. *J Neurosci* 18: 8111–8125, 1998.

**McBain CJ, Fisahn A.** Interneurons unbound. *Nat Rev Neurosci* 2: 11–23, 2001.

**McCormick DA, Connors BW, Lighthall JW, Prince DA.** Comparative electrophysiology of pyramidal and sparsely spiny stellate neurons of the neocortex. *J Neurophysiol* 54: 782–806, 1985.

**Merchant H, Naselaris T, Georgopoulos AP.** Dynamic sculpting of directional tuning in the primate motor cortex during three-dimensional reaching. *J Neurosci* 28: 9164–9172, 2008.

**Mitchell JF, Sundberg KA, Reynolds JH.** Differential attention-dependent response modulation across cell classes in macaque visual area V4. *Neuron* 55: 131–141, 2007.

**Moody SL, Wise SP, di Pellegrino G, Zipser D.** A model that accounts for activity in primate frontal cortex during a delayed matching-to-sample task. *J Neurosci* 18: 399–410, 1998.

**Mormann F, Kornblith S, Quiroga RQ, Kraskov A, Cerf M, Fried I, Koch C.** Latency and selectivity of single neurons indicate hierarchical processing in the human medial temporal lobe. *J Neurosci* 28: 8865–8872, 2008.

**Mountcastle VB, Talbot WH, Sakata H, Hyvarinen J.** Cortical neuronal mechanisms in flutter-vibration studied in unanesthetized monkeys. Neuronal periodicity and frequency discrimination. *J Neurophysiol* 32: 452–484, 1969.

**Mruczek RE, Sheinberg DL.** Context familiarity enhances target processing by inferior temporal cortex neurons. *J Neurosci* 27: 8533–8545, 2007a.

**Mruczek RE, Sheinberg DL.** Activity of inferior temporal cortical neurons predicts recognition choice behavior and recognition time during visual search. *J Neurosci* 27: 2825–2836, 2007b.

**Murray PD, Keller A.** Somatosensory response properties of excitatory and inhibitory neurons in rat motor cortex. *J Neurophysiol* 106: 1355–1362, 2011.

**Niell CM, Stryker MP.** Highly selective receptive fields in mouse visual cortex. *J Neurosci* 28: 7520–7536, 2008.

**Nowak LG, Azouz R, Sanchez-Vives MV, Gray CM, McCormick DA.** Electrophysiological classes of cat primary visual cortical neurons in vivo as revealed by quantitative analyses. *J Neurophysiol* 89: 1541–1566, 2003.

**Nowak LG, Sanchez-Vives MV, McCormick DA.** Lack of orientation and direction selectivity in a subgroup of fast-spiking inhibitory interneurons: cellular and synaptic mechanisms and comparison with other electrophysiological cell types. *Cereb Cortex* 18: 1058–1078, 2008.

**Olshausen BA, Field DJ.** Sparse coding of sensory inputs. *Curr Opin Neurobiol* 14: 481–487, 2004.

**Op De Beeck H, Vogels R.** Spatial sensitivity of macaque inferior temporal neurons. *J Comp Neurol* 426: 505–518, 2000.

**Peters A, Jones EG.** (Editors). *Cellular Components of the Cerebral Cortex*. New York: Plenum, 1984.

**Rainer G, Miller EK.** Effects of visual experience on the representation of objects in the prefrontal cortex. *Neuron* 27: 179–189, 2000.

**Ramón y Cajal S.** Estudios sobre la corteza cerebral humana. I. Corteza visual. *Revista Trimestral Micrográfica* 4: 1–63, 1899.

**Rao SG, Williams GV, Goldman-Rakic PS.** Isodirectional tuning of adjacent interneurons and pyramidal cells during working memory: evidence for microcolumnar organization in PFC. *J Neurophysiol* 81: 1903–1916, 1999.

**Robinson DA.** A method of measuring eye movement using a scleral search coil in a magnetic field. *IEEE Trans Biomed Eng* 10: 137–145, 1963.

**Rolls ET, Aggelopoulos NC, Zheng F.** The receptive fields of inferior temporal cortex neurons in natural scenes. *J Neurosci* 23: 339–348, 2003.

**Rolls ET, Tovee MJ.** The responses of single neurons in the temporal visual cortical areas of the macaque when more than one stimulus is present in the receptive field. *Exp Brain Res* 103: 409–420, 1995.

**Runyan CA, Schummers J, Van Wart A, Kuhlman SJ, Wilson NR, Huang ZJ, Sur M.** Response features of parvalbumin-expressing interneurons suggest precise roles for subtypes of inhibition in visual cortex. *Neuron* 67: 847–857, 2010.

**Sheinberg DL, Logothetis NK.** Noticing familiar objects in real world scenes: the role of temporal cortical neurons in natural vision. *J Neurosci* 21: 1340–1350, 2001.

**Simons DJ, Carvell GE.** Thalamocortical response transformation in the rat vibrissa/barrel system. *J Neurophysiol* 61: 311–330, 1989.

**Sohya K, Kameyama K, Yanagawa Y, Obata K, Tsumoto T.** GABAergic neurons are less selective to stimulus orientation than excitatory neurons in layer II/III of visual cortex, as revealed by in vivo functional $Ca^{2+}$ imaging in transgenic mice. *J Neurosci* 27: 2145–2149, 2007.

**Sugase Y, Yamane S, Ueno S, Kawano K.** Global and fine information coded by single neurons in the temporal visual cortex. *Nature* 400: 869–873, 1999.

**Swadlow HA.** Efferent neurons and suspected interneurons in S-1 vibrissa cortex of the awake rabbit: receptive fields and axonal properties. *J Neurophysiol* 62: 288–308, 1989.

**Swadlow HA.** Fast-spike interneurons and feedforward inhibition in awake sensory neocortex. *Cereb Cortex* 13: 25–32, 2003.

**Tamura H, Kaneko H, Kawasaki K, Fujita I.** Presumed inhibitory neurons in the macaque inferior temporal cortex: visual response properties and functional interactions with adjacent neurons. *J Neurophysiol* 91: 2782–2796, 2004.

**Tanigawa H, Fujita I, Kato M, Ojima H.** Distribution, morphology, and gamma-aminobutyric acid immunoreactivity of horizontally projecting neurons in the macaque inferior temporal cortex. *J Comp Neurol* 401: 129–143, 1998.

**Thompson KG, Hanes DP, Bichot NP, Schall JD.** Perceptual and motor processing stages identified in the activity of macaque frontal eye field neurons during visual search. *J Neurophysiol* 76: 4040–4055, 1996.

**Toledo-Rodriguez M, Gupta A, Wang Y, Wu CZ, Markram H.** Neocortex: basic neuron types. In: *The Handbook of Brain Theory and Neural Networks*, edited by Arbib MA. Cambridge, MA: MIT Press, 2003, p. 719–725.

**Towe AL, Harding GW.** Extracellular microelectrode sampling bias. *Exp Neurol* 29: 366–381, 1970.

**Vigneswaran G, Kraskov A, Lemon RN.** Large identified pyramidal cells in macaque motor and premotor cortex exhibit "thin spikes": implications for cell type classification. *J Neurosci* 31: 14235–14242, 2011.

**Wang Y, Fujita I, Murayama Y.** Neuronal mechanisms of selectivity for object features revealed by blocking inhibition in inferotemporal cortex. *Nat Neurosci* 3: 807–813, 2000.

**Wilson FA, O'Scalaidhe SP, Goldman-Rakic PS.** Functional synergism between putative gamma-aminobutyrate-containing neurons and pyramidal neurons in prefrontal cortex. *Proc Natl Acad Sci USA* 91: 4009–4013, 1994.

**Woloszyn L, Sheinberg DL.** Effects of long-term visual experience on responses of distinct classes of single units in inferior temporal cortex. *Neuron* 74: 193–205, 2012.

**Yokoi I, Komatsu H.** Putative pyramidal neurons and interneurons in the monkey parietal cortex make different contributions to the performance of a visual grouping task. *J Neurophysiol* 104: 1603–1611, 2010.

**Zoccolan D, Kouh M, Poggio T, DiCarlo JJ.** Trade-off between object selectivity and tolerance in monkey inferotemporal cortex. *J Neurosci* 27: 12292–12307, 2007.